REPORT DOCUMENTATION PAGE

Form Approved
OMB No. 0704-0188

1. REPORT DATE *(DD-MM-YYYY)*
06-05-2004

REPRINT

4. TITLE AND SUBTITLE
Parameterizing the Wind 3DP Hat Flux Electron Data

5a. CONTRACT NUMBER

5b. GRANT NUMBER

5c. PROGRAM ELEMENT NUMBER
61102F

5d. PROJECT NUMBER
2311

5e. TASK NUMBER
RD

5f. WORK UNIT NUMBER
A1

6. AUTHOR(S)
S.W. Kahler, N.U. Crooker* and D.E. Larson**

7. PERFORMING ORGANIZATION NAME(S) AND ADDRESS(ES)
Air Force Research Laboratory/VSBXS
29 Randolph Road
Hanscom AFB MA 01731-3010

20040511 019

9. SPONSORING / MONITORING AGENCY NAME(S) AND ADDRESS(ES)

10. SPONSOR/MONITOR'S ACRONYM(S)
AFRL/VSBXS

11. SPONSOR/MONITOR'S REPORT NUMBER(S)
AFRL-VS-HA-TR-2004-1063

12. DISTRIBUTION / AVAILABILITY STATEMENT
Approved for Public Release; Distribution Unlimited.

*Center for Space Physics, Boston Univ, MA; **Space Sciences Lab, Univ Calif, Berkeley, CA

13. SUPPLEMENTARY NOTES
REPRINTED FROM: SOLAR WIND TEN (EDITORS M. VELLI ET AL), AIP CONFERENCE PROCEEDINGS, Vol 679, NEW YORK, 2003.

14. ABSTRACT

Abstract. Solar wind heat flux (HF) electrons are valuable as tracers of the interplanetary magnetic field (IMF) topology, distinguishing positive from negative solar polarities and indicating the presence of magnetically closed CMEs when the flows are counterstreaming. All past applications of heat fluxes to determine field topologies have been based on visual inspection of color spectrograms of electron pitch angle distributions (PADs). However, HF PADs can take a range of shapes and amplitudes, which challenges the visual analysis. We now take a quantitative approach to HF analysis by parameterizing the HF PADs of the UC Berkeley 3DP data with a Fourier harmonic analysis. We have calculated the harmonic cosine coefficients A_0 through A_4 for a five-year period of the Wind 3DP data set with a 10-min time resolution. With these data we intend to derive quantitative criteria for unidirectional and bi-directional flows and other possible diagnostics of interplanetary field dynamics or configurations. Some initial considerations and results of the 3DP parameterization are presented.

15. SUBJECT TERMS
Interplanetary magnetic fields
Sources of the solar wind
Solar wind plasma
Charged particle motion

16. SECURITY CLASSIFICATION OF: a. REPORT	b. ABSTRACT	c. THIS PAGE	17. LIMITATION OF ABSTRACT	18. NUMBER OF PAGES	19a. NAME OF RESPONSIBLE PERSON
UNCLAS	UNCLAS	UNCLAS	SAR	4	S. W. Kahler
					19b. TELEPHONE NUMBER *(include area code)* 781-377-9665

Standard Form 298 (Rev. 8-98)
Prescribed by ANSI Std. 239.18

AFRL-VS-HA-TR-2004-1063

DISTRIBUTION STATEMENT A
Approved for Public Release
Distribution Unlimited

Parameterizing the Wind 3DP Heat Flux Electron Data

S.W. Kahler*, N.U. Crooker† and D.E. Larson**

Space Vehicles Directorate, Air Force Research Laboratory
†*Center for Space Physics, Boston University*
***Space Sciences Laboratory, University of California*

Abstract. Solar wind heat flux (HF) electrons are valuable as tracers of the interplanetary magnetic field (IMF) topology, distinguishing positive from negative solar polarities and indicating the presence of magnetically closed CMEs when the flows are counterstreaming. All past applications of heat fluxes to determine field topologies have been based on visual inspection of color spectrograms of electron pitch angle distributions (PADs). However, HF PADs can take a range of shapes and amplitudes, which challenges the visual analysis. We now take a quantitative approach to HF analysis by parameterizing the HF PADs of the UC Berkeley 3DP data with a Fourier harmonic analysis. We have calculated the harmonic cosine coefficients A_0 through A_4 for a five-year period of the Wind 3DP data set with a 10-min time resolution. With these data we intend to derive quantitative criteria for unidirectional and bi-directional flows and other possible diagnostics of interplanetary field dynamics or configurations. Some initial considerations and results of the 3DP parameterization are presented.

1. INTRODUCTION

Solar-wind heat flux electrons have provided a powerful tool for determining the solar magnetic polarities of the interplanetary magnetic field (IMF) [1, 2]. Those electrons, with energies $E \geq 80$ eV, stream antisunward parallel to positive polarity field lines and antiparallel to negative polarity field lines, independently of the local field directions. By determining whether the pitch angle distribution (PAD) is concentrated at 0° or 180°, i.e., parallel or antiparallel to the field, respectively, we can establish the solar polarities of the IMF. It is possible to detect fields locally turned back to the Sun or, with bidirectional electron (BDE) flows, the closed fields of ICMEs (Figure 1).

The first plots of HF flow directions were based on a solar-pointing coordinate system and required a visual comparison of the observed IMF direction with the HF flow direction to estimate the PAD (e.g., [3, 4]). HF plots from current spacecraft are done in a coordinate system fixed on the IMF direction, which immediately yields the PAD. While simplifying the analysis, it does not avoid the considerable variation among PADs (e.g., [5, 6]) which sometimes leaves the net HF flow direction or the presence of bidirectionality [3] in doubt. In addition, the PADs are usually plotted with a color table which may or may not be normalized for the total number of electrons observed in the PADs. The recent reports of HF depletions at 90° PA [6, 7] suggest another possible HF diagnostic of IMF structure, but the identification and magnitude of these features is compromised when we are limited to a subjective analysis based on the color-coded PAD contour plots.

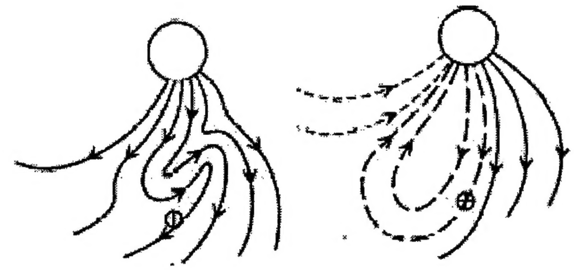

FIGURE 1. Schematic illustrations of open fields of the IMF locally turned back to the Sun (left) and a closed field topology of an ICME (right). The polarity of the turned back fields can be inferred from the primary direction of the HF PAD, and the closed fields are indicated by bidirectional HF PADs.

2. ANALYSIS

To provide quantitative diagnostics for the different types of PADs, we are beginning to analyze the 3DP [8] HF electron PAD data in terms of Fourier cosine harmonics using the following least-squares fit to the

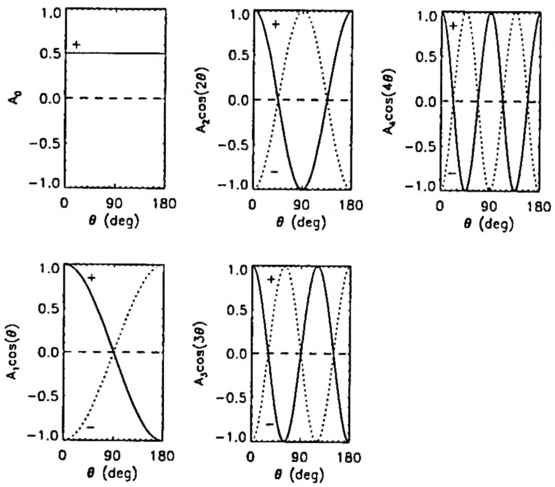

FIGURE 2. Graphical presentations of the terms of the fits to equation (1). The A_2 and A_4 terms are important for bidirectionality and depletions, respectively. Dotted lines show profiles of negative values.

13-point HF PAD intensities

$$\log I(\theta) = A_0 + A_1\cos(\theta) + A_2\cos(2\theta) + A_3\cos(3\theta) + A_4\cos(4\theta)$$

where θ is the PA, which ranges from 0° to 180°. Because of the large dynamic range of the HF intensities, we do a logarithmic rather than a linear fit to the intensity I. Plots of the five harmonic terms as functions of θ are shown in Figure 2. Note that a bidirectional flow [3] should have a significant positive A_2 term and a depletion [6, 7] a significant negative A_4 term. We have now calculated the five harmonic components for all the WIND 3DP HF data from 1995 through 1999 in 10-min intervals for electron energies of 125, 250, and 500 eV.

To examine the signatures of the various A_n we selected 3 days with very different characteristic PADs (Figure 3) : 1 Jan 1995 has a poorly defined and relatively flat PAD; 3 Aug 1996 has a well defined 0° PAD and 25 Jun 1998 has a BDE PAD, with peaks at 0° and 180°, most of the day.

2.1. A_2 and the BDE Diagnostic

A_2 is the key parameter for detecting BDE flows. Figure 4 shows the plot of log $I(\theta)$ for various ratios of A_2/A_1 when A_2 and $A_1 > 0$. We see that bidirectionality is not apparent until $A_2/A_1 \sim 1$. Selecting an arbitrary value of A_2/A_1 to define periods of bidirectionality will be a critical choice for our anticipated 3DP survey. We note that Richardson and Reames [9] chose $A_2/A_1 > 0.8$ for their survey of bidirectional energetic ($\sim$ 1 MeV) ion

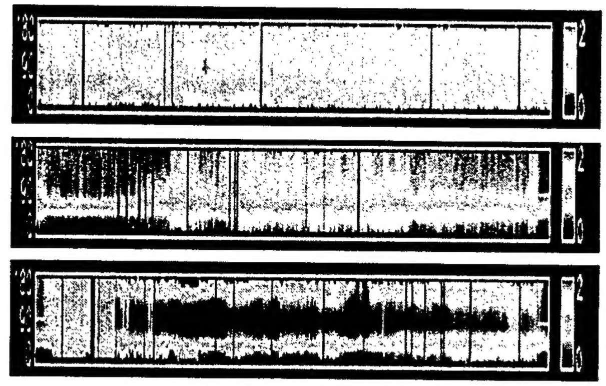

FIGURE 3. Three days with very different 3DP 260 eV electron PADs: top, flat PADs of 1 Jan 1995; middle, directed PADs of 3 Aug 1996; bottom, BDE PADs of 25 Jun 1998. The PA scales extend from 0° on the bottom to 180° at the top.

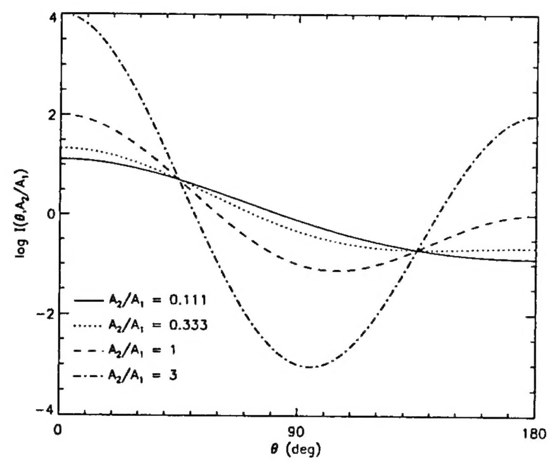

FIGURE 4. Plot of log $I(\theta)$ for four different ratios of $|A_2|/|A_1|$ with other A_n set to 0.

flows.

Our goal here is to get a general impression of the parametric variations among the three days with the very different PADs as determined by eye. We plotted $\log(|A_2|)$ against $\log(|A_1|)$ for the 10-min intervals of each of the three selected days and at each of the three electron energies used in the harmonic analysis. Figure 5 shows the results. The diagonal lines of the plots enable us to compare the magnitudes of A_2 with A_1. We see first that the plots are very similar for each of the three selected electron energies, suggesting that the particular energy range chosen as the standard for analysis is not critical. We also find that A_2, nearly always positive throughout each period, exceeds 0.2 for most of the BDE

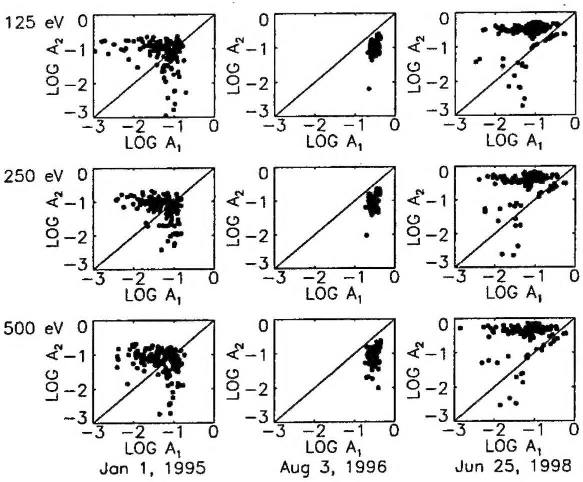

FIGURE 5. Plot of $\log(|A_2|)$ against $\log(|A_1|)$ for the three different electron energies and for the three different PAD distributions shown in Figure 3. The right column contains points from the day of obvious BDE PADs. Above the diagonal lines $|A_2| > |A_1|$.

PAD points, but is rarely that large in the flat and directed PADs. In addition, while $A_2 > A_1$ in the BDE PADs and $A_2 < A_1$ in the directed PADs, perhaps as expected, we also find that usually $A_2 > A_1$ in the flat PADs. As a possible strategy for selecting criteria for BDEs, we could plot A_2 versus A_1 data points for the whole 1995-1999 period, looking for a separate population of points in the approximate ranges defined by $A_2 \geq A_1$ and $A_2 > 0.2$.

2.2. A_3 and the HF Flow Diagnostic

The most important goal in this analysis is to determine when we have a sufficiently clearly defined HF flow direction to decide the IMF polarity. From Figure 2 we see that when A_3 and A_1 have the same sign and $A_3 > A_1$, the flow direction is reversed from that indicated by A_1 alone. In Figure 6 we show plots of $\log(|A_3|)$ against $\log(|A_1|)$. Points above the diagonal line indicate cases in which A_3 is large enough to result in a net HF flow reversed from that of A_1 if both terms have the same sign. A substantial number of points in the flat and BDE PADs suggest such reverse flows. However, a complication here is that about 20-30% of the A_3 points have signs opposite those of the corresponding A_1 values and therefore enhance the net HF flow. In addition, large values of A_2 could act to diminish the net HF flows determined from the A_1 and A_3 values alone.

The ambiguities involved in trying to sort out a set of relationships among A_1, A_2, and A_3 suggest that a better approach may be simply to calculate the net HF

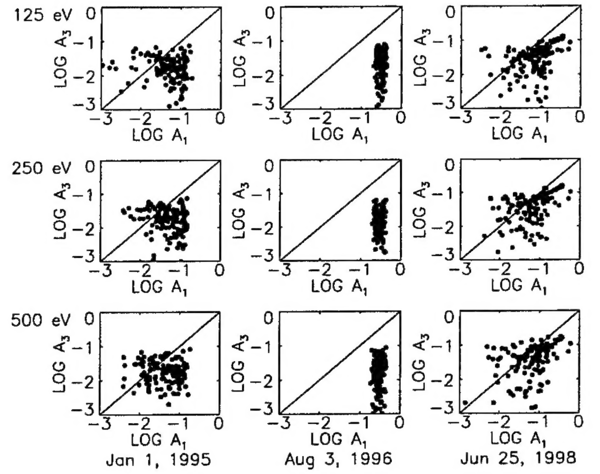

FIGURE 6. Plots of $\log(|A_3|)$ against $\log(|A_1|)$ with the same format as in Figure 5.

Q_e over all electron energies. We have done this and show the plots for the three days in Figure 7. The red trace is Q_e parallel to the magnetic field direction, and the purple and green traces show the Q_e in directions orthogonal to the IMF. The magnitudes of the purple plots, calculated along the axis perpendicular to the plane of the IMF direction and the Sun, are comparable to the uncertainties of the calculated Q_e along the IMF and can be used as filters for valid HF flow directions. In particular, we see that for much of the 1 Jan 1995 flat PAD plot the magnitudes of many of the perpendicular HF points are comparable to the matching points of the parallel points, suggesting poorly defined HF directions. On the other hand, the parallel HF is much greater than the perpendicular HFs for all of the directed PAD plot of 3 August 1996. Note that the HF calculation used here does not produce the systematic 20° deviations between the Q_e and B directions found by Salem et al. [10].

2.3. A_4 and Depletions

The inclusion of the A_4 harmonic shown in Figure 2 enables us to look for the cases of depletions [6, 7], the significant decreases symmetrically centered on 90° PA. Figure 8 shows plots of $\log(A_4)$ against $\log(A_2)$ with the positive and negative values of $\log(A_4)$ plotted on separate panels. Recall that A_2 is nearly always positive in our selected data sets, producing a broad PAD depression at 90°. A negative A_4 term is consistent with the further narrow, symmetric depression at 90° that characterizes depletions. In most cases of Figure 8 $|A_4| < |A_2|$, and A_4 is negative (bottom panels). While these limited

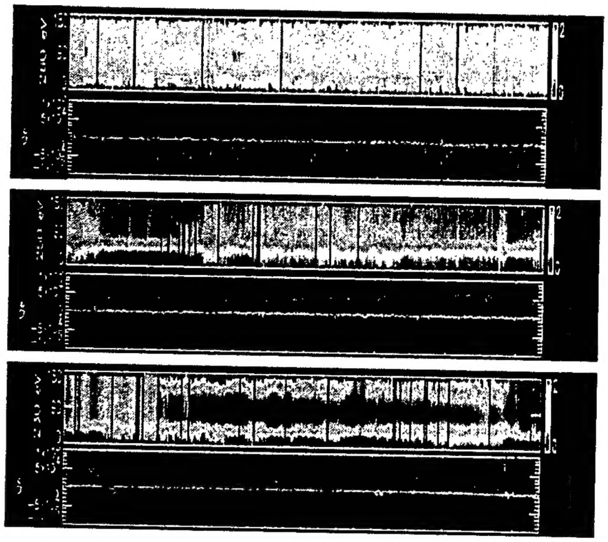

FIGURE 7. Pairs of 3DP 260 eV PADs (top) and Q_e (bottom) for the same three days of Figure 3. In the Q_e plots the red trace shows Q_e along the IMF direction, the purple along a perpendicular to the plane of the IMF direction and the Sun and the green along the third orthogonal axis.

results suggest that depletions may be defined by the criteria that $A_4 < 0$ and $|A_4| > 0.5 \times |A_2|$, a much larger survey of the 3DP data parameters will be required to justify those criteria.

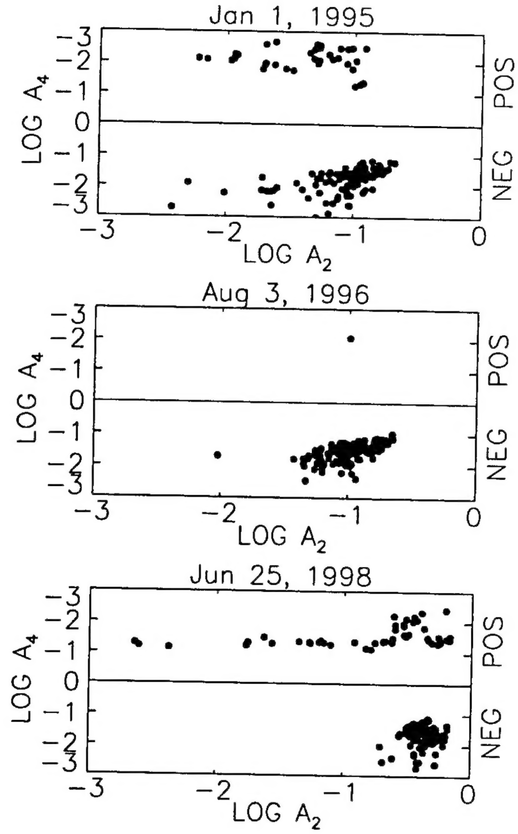

FIGURE 8. Plots of $\log(A_4)$ versus $\log(A_2)$ for the three days of the study. Here we distinguish between the positive (upper panels) and negative (lower panels) signs of A_4. The predominately negative values of A_4 are expected when PAD depletions [6, 7] occur.

3. DISCUSSION

The five-year data base of the 3DP HF electron data has been analyzed in terms of the first four Fourier cosine coefficients over 10-min averages. We intend to develop quantitative criteria for the A_n coefficients that will enable us to determine IMF solar polarities and to find periods of BDEs and depletions. In this initial work we have examined characteristic parametric tradeoffs among the A_n for three selected days with very different kinds of PADs.

ACKNOWLEDGMENTS

This work was supported by NASA under grants NAG5-10856 at Boston University and DPR W-19,926 at the Air Force Research Laboratory. We thank A. Ling for generating the computer plots.

REFERENCES

1. Kahler, S., and Lin, R.P., *Geophys. Res. Let.*, **21**, 1575, 1994.
2. Kahler, S.W., in *Coronal Mass Ejections*, edited by N. Crooker et al., Geophys. Mon. 99, AGU, p.197, 1997.
3. Gosling, J.T., et al., *J.Geophys. Res.*, **92**, 8519, 1987.
4. Kahler, S.W., Crooker, N.U., and Gosling, J.T., *J. Geophys. Res.*, **101**, 24373, 1996.
5. Feldman, W.C., et al., *Geophys. Res. Let.*, **26**, 2613, 1999.
6. Gosling, J.T., Skoug, R.M., and Feldman, W.C., *Geophys. Res. Let.*, **28**, 4155, 2001.
7. Gosling, J.T., Skoug, R.M., Feldman, W.C., and McComas, D.J., *Geophys. Res. Let.*, in press, 2002.
8. Lin, R.P., et al., *Space Sci. Rev.*, **71**, 125, 1995.
9. Richardson, I.G., and Reames, D.V., *Ap. J. Suppl. Ser.*, **85**, 411, 1993.
10. Salem, C., et al., *J. Geophys. Res.*, **106**, 21701, 2001.